ISBN: 978-3-95450-260-8 ISSN: 2673-5547 doi: 10.18429/JACoW-HIAT2025-TUZ02

PRIMARY BEAM DEVELOPMENT FOR FRIB EXPERIMENTS*

T. Maruta†, K. Fukushima, A. Gonzalez, K. Hwang, P.N. Ostroumov, A.S. Plastun, T. Zhang, Q. Zhao, Facility for Rare Isotope Beams, Michigan State University, East Lansing, USA

Content from this work may be used under the terms of the CC BY 4.0 licence (© 2025). Any distribution of this work must maintain attribution to the author(s), title of the work, publisher, and DOI.

Abstract

Since starting the user operation of Facility for Rare Isotope Beams (FRIB) at Michigan State University in May 2022, the driver linac has provided more than a dozen ion beam species from Oxygen to Uranium to the production target. FRIB routinely provided 20 kW primary beams on target since March 2025, which is a factor of 20 higher than at the beginning of the scientific user operation. In this presentation, the recent progress of FRIB driver linac beam development, a discussion of efficient primary beam tuning procedures based on physics applications, and accelerator improvement projects for low-loss accelerator will be discussed.

INTRODUCTION

FRIB is a heavy ion accelerator facility constructed at Michigan State University under the corporate agreement with the U.S. Department of Energy Office of Science to support the Office of Nuclear Physics mission. The facility is comprised of the driver linac, fragment separator, and experimental area including 6 MeV/u reacceleator. Construction was completed in January 2022, and user operation started in May 2022.

The driver linac is designed to provide a 400 kW continuous wave beam to the production target [1]. The required primary ions are generated in the Electron Cyclotron Resonance (ECR) source, selected after a 90° bend, and transported to the accelerator tunnel through 24-meter-long Low Energy Beam Transport (LEBT). The beam is accelerated by Radio Frequency Quadrupole (RFQ) and the following three linac segments (LS1, LS2 and LS3). The beam acceleration is provided by four types of Superconducting (SC) RF cavities with optimal β from 0.041 to 0.54. For the beam focusing in the cryomodules, we use SC solenoids equipped with horizontal and vertical steering coils. The layout of the linac is shown in Fig. 1. For a detailed description of the linac structure, we refer to earlier publications, for example, [2]. The beam accelerated by the LS1 interacts with the charge stripper, which is a highly beneficial technique for heavy ion accelerators. The electrons are stripped off the ions while passing through a thin material, which boosts the charge-to-mass ratio (q/A) of beams for efficient acceleration. FRIB has developed 20 – 30 μm thick liquid lithium film as the stripper (LLCS) [3] because of its high capability of thermal load and radiation resistance. Due to the stochastic nature of the stripping process, the output beam is distributed to several charge states. In most cases, the charge state distribution is a Gaussian function, and the fraction of beam intensity in a single charge state is low. Table 1 shows recently operated beams, including the stripping efficiencies measured in FRIB. The yield of the central charge state of the ^{238}U beam is only 21% of the initial intensity.

Table 1: Beam parameters during the recent beam operations. The stripping efficiencies were measured at 17 MeV/u for ^{124}Xe and ^{238}U, and 20 MeV/u for the rest of ions.

Ion	Charge states after stripper	Energy at the target [MeV/u]	Stripping efficiency 1q / Multi-q
^{48}Ca	19+, 20+	225	72% / 98%
^{58}Ni	26+, 27+	250	66% / 94%
^{64}Zn	28+, 29+	240	71% / 88%
^{82}Se	32+, 33+	200	74% / 88%
^{124}Xe	48+ ~ 50+	240	30% / 76%
^{238}U	73+ ~ 77+	177	21% / 83%

To provide higher stripping efficiency, the FRIB linac has been designed to accelerate multiple charge states simultaneously. To avoid the growth of the effective emittance due to trajectories' displacement, the bending systems in FS1, FS2 and BDS have been designed to satisfy achromat conditions and merge all charge states' central trajectories after the bends [4]. The aperture in the dispersive plane is sufficient to accept five charge states of the uranium beam with charge state spread $\Delta q/q_{cen}$, equal to 5.3%. The multi-charge acceleration substantially reduces the deposited power of unwanted charge states on the Charge Selection Slits (CSS) installed after the first bending dipole in the FS1 and reduces required radiation shielding. In the present CSS, absorbed beam power at the single spot is limited to 500 W. For example, after the stripping, the $^{48}Ca^{19+}$ fraction is 26% and the 500 W limit corresponds to approximately 13 kW of $^{48}Ca^{20+}$ only delivered to the target.

The beam time of most experiments is less than a week. Each experiment requires different primary ion species and energy on the target. Therefore, shortening the primary beam tuning time through efficient procedures is essential to provide more time for science.

* Work supported by the U.S. Department of Energy Office of Science under Cooperative Agreement DE-SC0023633, the State of Michigan, and Michigan State University. Also, part of this work is supported by the U.S. Department of Energy Office of Nuclear Physics under Award Number DE-SC0025531.
† maruta@frib.msu.edu

ISBN: 978-3-95450-260-8 ISSN: 2673-5547 doi: 10.18429/JACoW-HIAT2025-TUZ02

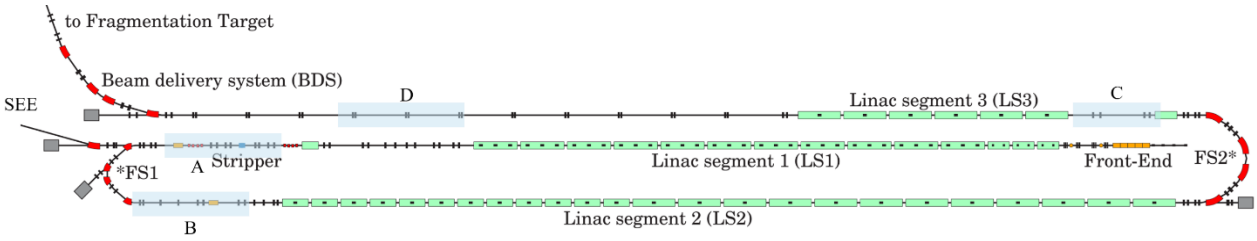


Figure 1: Layout of the FRIB driver linac.

NEW BEAM DEVELOPMENT

The development of a new primary beam starts with a pre-calculation of the accelerator setting by simulation tools. The RF cavities' from MEBT to the target are calculated by a model-based Instant Phase Setting (IPS) application [5]. The amplitude and synchronous phase of each cavity are optimized to meet the energy requirement and provide sufficient stability area in the longitudinal phase space. The calculated RF cavities' settings are loaded to 3D beam envelope code FLAME to calculate required focusing fields. The solenoids in the acceleration segments LS1 and LS2 are set to provide the transverse phase advance per period below 90°. Then, five sections of quadrupoles (upstream of the LS1, upstream of the LS2, upstream of the stripper, FS2 and BDS sections) are optimized to match Courant-Snyder (CS) parameters of all charge states simultaneously to the following beam optics. The magnets' setting is registered to the application "Settings Manager" [6] and matched CS parameters are registered to the beam envelope tuning application in the accelerator control network.

The calculated setting is applied to beamline devices at the beginning of Primary beam Development Time (PDT). The latter includes beam central trajectory tuning and envelope matching along the linac. We typically conduct matching in 5 sections of the accelerator. RMS beam size is measured in each location by varying quadrupole settings to calculate the RMS CS parameters and calculate the optimum quadrupole setting to match all charge states simultaneously.

RECENT PROGRESS WITH LINAC TUNING

Since the start of the scientific user operation in May 2022, the beam power of the driver linac has gradually increased to 20 kW. Up to now, 13 stable isotope (^{18}O, ^{22}Ne, ^{28}Si, ^{36}Ar, ^{40}Ar, ^{48}Ca, ^{58}Ni, ^{64}Zn, ^{70}Zn, ^{82}Se, ^{124}Xe, ^{198}Pt, and ^{238}U) beams have been accelerated up to 300 MeV/u and delivered to the production target. In addition, seven isotope (^{16}O, ^{40}Ar, ^{86}Kr, ^{107}Ag, ^{129}Xe, ^{169}Tm, and ^{209}Bi) beams have been provided to the test station in the Single Event Experiment (SEE) beamline with energies ranging from 10 to 40 MeV/u.

Lithium Film Stage Feedback in Operation

We have observed the energy loss fluctuation at LLCS from the beginning of its operation. Figure 2 shows energy loss distribution for ^{124}Xe and ^{238}U beams. There are 3 ~ 5 meta-stable states of the lithium film thickness quickly jumping from one to another in a 0.1 s time scale. The energy feedback system has been developed, and it is in operation to stabilize the post-stripper energy and bunch timing by automatically adjusting the driven phase of the last cavity in LS1 with 0.1 s response time [7]. This feedback system helps us to control the longitudinal emittance growth due to longitudinal tails folded by non-linear fields in FS1 buncher cavities and minimize the beam losses in the LS2 cryomodules. The letter results in the temperature increase of cold beam pipes in the cryomodules. In the absence of the feedback, the beam losses in LS2 are increased, especially for the uranium beam, if the stripper film suddenly jumps to another meta-stable state of the lithium flow.

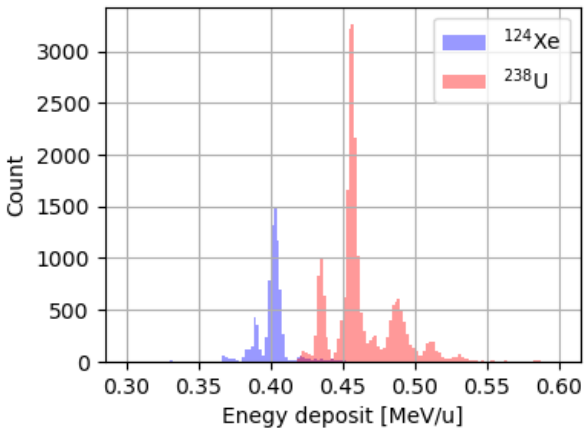


Figure 2: Distribution of energy loss at LLCS for ^{124}Xe (pale blue) and ^{238}U (pale red) beams without LLCS stage feedback.

Another feedback system has been implemented recently to stabilize the beam energy loss in the stripper. The feedback automatically moves the LLCS stage vertically, i.e. the beam spot on the film to correct the energy loss on the film once the energy loss varies more than 5% from the reference value which is set by an accelerator physicist during the PDT. The feedback response time is approximately tens of seconds. These two kinds of feedback systems stabilize the output beam energy, arrival timing, and stripper energy loss with two orders of different time scales. Figure 3 shows how the feedback worked in a recent operation. The energy loss (red) suddenly increased from 0.43 to 0.49 MeV/u at (a). The post stripper energy (green) changes accordingly but immediately returns to the original energy by adjusting the LS1 cavity's phase (blue). The

Content from this work may be used under the terms of the CC BY 4.0 licence (© 2025). Any distribution of this work must maintain attribution to the author(s), title of the work, publisher, and DOI.

ISBN: 978-3-95450-260-8 ISSN: 2673-5547 doi: 10.18429/JACoW-HIAT2025-TUZ02

Content from this work may be used under the terms of the CC BY 4.0 licence (© 2025). Any distribution of this work must maintain attribution to the author(s), title of the work, publisher, and DOI.

stage feedback recognized the change of energy loss at (b) and started moving the stage (purple). The motion of the stage continued for ~45 sec, and the LS1 cavity phase continuously changed during the stage to keep the post-stripper energy through the end of motion at (c). Note that the energies on this plot are average for the last one second, so the energy feedback response is quicker than the plot. By activating these feedbacks simultaneously, the temperature increase in LS2 crymodules is reduced to nearly half, which unleashes 50 kW operation for ^{238}U and even higher for lighter ions.

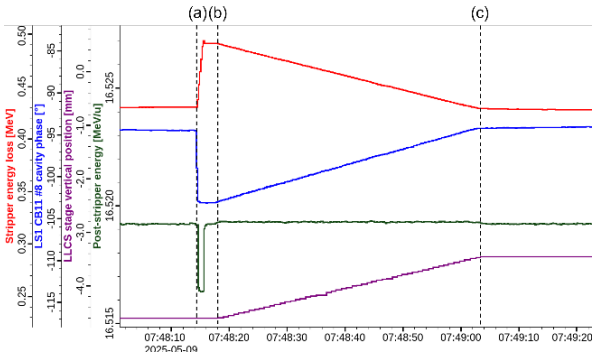


Figure 3: The post-stripper energy and energy loss at LLCS are controlled by energy and LLCS stage feedbacks. The energies (red and green) on this plot are averages for the last 1 sec, so the actual energy change is quicker than this plot.

Acceleration of Five Charge States of Uranium Beam

The world record of 10.4 kW was demonstrated in December 2023 by accelerating three charge states (3-q, 74+, 75+, 76+) [8] to 177 MeV/u, resulting in 58% stripping efficiency. While a 10 kW beam has been stably delivered to the target for new isotope search, there were relatively high beam losses in the FS2 and BDS, and temperature sensors in the LS2 showed a 0.4 K increase. Note that at that time, the stripper stage feedback was not available.

Further improvements of the ^{238}U beam optics was conducted in June 2024. The RF cavities' setting was optimized to provide stability for five charge states of uranium. The differences between the central trajectories of all charge states are mitigated to be within 1.5 mm in non-dispersive sections by carefully tuning dipoles, quadrupoles and sextupoles in the bending systems. Also, the simultaneous 5-q transverse matchings were performed upstream of the LS2, LS3, and BDS sections. This tune accepts 5-q (73+ to 77+), and stripping efficiency was increased to 83%. During the ramping up of the beam power to the target, the beam image of 5-q on the 2.1 mm thick static carbon target was taken at 500 W as shown in Fig. 4. No beamlets were observed on the image, and RMS beam size on both horizontal and vertical directions is below 0.5 mm. This optics is our current reference setting and has been employed for the recent 20 kW operations with trajectories' corrections and some tunings in the front end to compensate for the beam profile variation from the ECR ion source.

The ICs, Neutron Detectors (NDs) and thermal sensor signals during the recent 20 kW operation are shown in Fig. 5 (top). Their signals from 220 to 240 meters come from the stripper and CSS. ICs in FS2 and BDS detect signals below 20 mR/hr, which is less by a factor of 5 compared to 3-q operation in 2023.

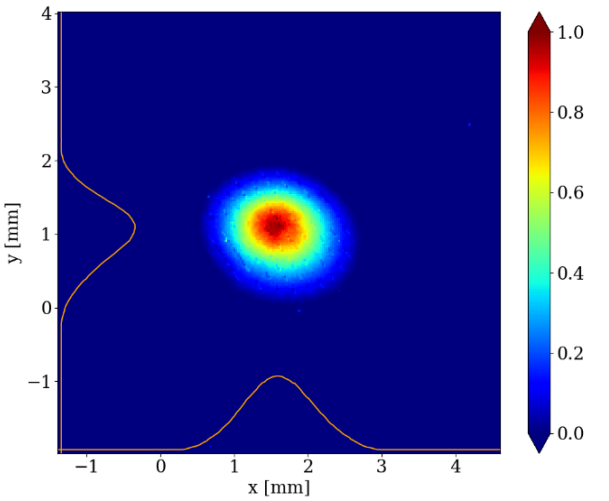


Figure 4: Thermal image of 5-q ^{238}U beam image on the static fragmentation target. The temperature range is scaled from 0 to 1.

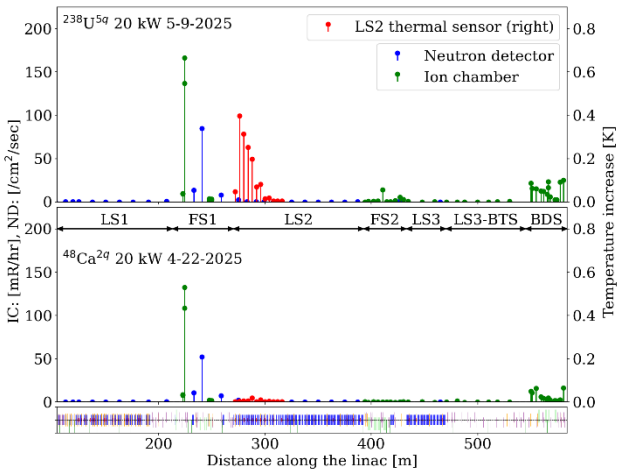


Figure 5: Beam loss signals during 20 kW ^{238}U^{5q} (top) and ^{48}Ca^{2q} (bottom). The Neutron Detectors (NDs, blue), ion chambers (ICs, green), and thermal sensors in LS2 cryomodules (red) are shown. The signals from 220 to 240 m come from the stripper and the CSS.

Although the beam losses have been successfully mitigated, significant emittance growth was observed during the transverse beam tunings. Figure 6 shows the measured normalized emittance of each charge state. The emittance of 73+ is approximately doubled at LS3 entrance and further increased by ~3.5 times at BDS upstream. 74+ also shows a factor of two growth from LS3 to BDS but much less than 73+. The emittances of other charge states remain nearly constant. The SC solenoids are installed for LSs transverse focusing, which can mix up the horizontal and

ISBN: 978-3-95450-260-8 ISSN: 2673-5547 doi: 10.18429/JACoW-HIAT2025-TUZ02

vertical emittance in 4D phase space if the beam is mismatched. The number of quadruples available for the matching is ten for the section upstream of the LS2 and eight for LS3, which is less than a number of quadrupoles available in the BDS. This has motivated us to plan the installation of additional quadrupoles in these areas to better match multi-q beams.

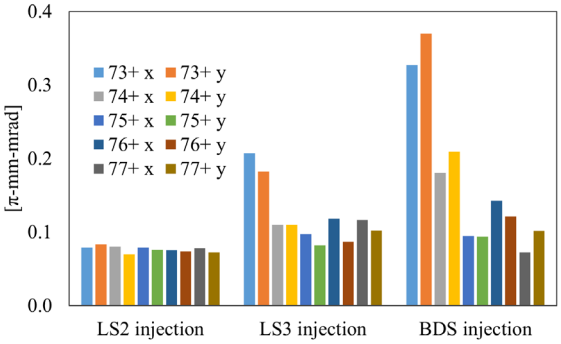


Figure 6: Normalized transverse RMS emittances for each charge state of $^{238}U^{5q}$ beam measured by quadrupole scans.

Acceleration of Two Charge States of Calcium Beam

As mentioned, 2-q acceleration is essential for the Ca beam to deliver 20 kW or higher to the target while adhering to the single spot power limit of 500 W at the CSS. 2-q beam development started from ^{82}Se beam, which is the least $\Delta q/q_{ave}$ in our beam list, and then gradually extended to the Ca beam with the highest charge spread, 5.1%, close to the design limit of the bending systems.

In the initial Ca beam development, substantial emittance growth has been observed for 20+ through LS2 and LS3. The solenoid setting in LSs was originally developed for 20+ acceleration, and increased by 2.6% for 2-q acceleration. This setting has been kept even when cavity settings were changed for different velocity profiles in LS2, which resulted in high transverse phase advance per period and irregular descent along the LS2, as shown with the blue line in Fig. 7. Currently, we speculate that the higher solenoid fields negatively impact the emittance projections into x-x' and y-y' phase spaces for the magnetized beam produced in the ECR. The solenoid setting was re-calculated so that the phase advance starts at 90° and adiabatically changes to ~35° as the green line in Fig. 7. After the beam development with the new solenoid setting, the emittance growth is mitigated, and beam losses at 20 kW are below 20 mR/hr in BDS.

ACCELERATOR IMPROVEMENT PROJECTS

Recent 20 kW operations with Ca, Ni, Zn, Se, Xe, and U beams show that the linac's beam losses are tolerable for > 50 kW if they increase linearly with the beam intensity. FS1 upgrade projects are underway to further reduce the beam losses, especially those related to the lithium stripper, and prepare the linac for acceleration of beams above 50 kW.

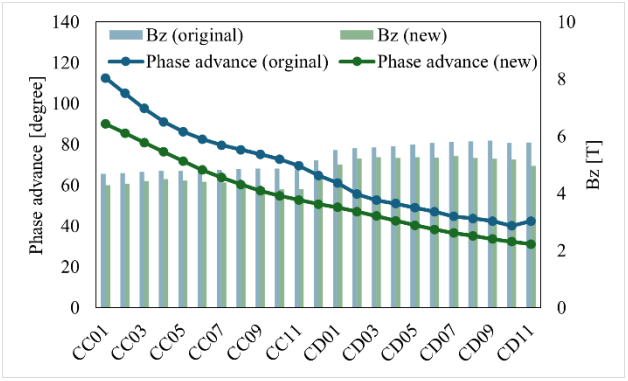


Figure 7: LS2 Transverse phase advance per period and solenoids' field in each cryomodule in original (blue) and new optics (green).

Large Bore Quadrupoles around the Stripper

The thin liquid lithium film has limited thickness uniformity. Because beam energy loss is proportional to the thickness of the film, beam energy spread increases with larger thickness nonuniformity, resulting in higher longitudinal emittance growth. Consequenly, the longitudinal halo causes beam losses in the LS2.

Improving the film thickness uniformity is essential for reducing the beam losses in the cryomodules. To mitigate the nonuniformity on the beam spot, we have tuned quadrupoles upstream of the stripper in every PDT so that the beam size on the stripper is as small as possible with RMS beam size in quadrupoles below ¼ of aperture to avoid any beam losses. The black line in Fig. 8 shows the correlation between beam size and the standard deviation of the thickness of the beam spot when the average thickness on the beam spot is 1.0 mg/cm^2, which is evaluated using the thickness distribution measurements [3]. The RMS beam size on the stripper film has typically been 0.5 mm in recent operations, and the thickness nonuniformity is 0.12 mg/cm^2. The nonuniformity exponentially increases as a function of the beam size, so it is crucial to maintain beam rms size on the stripper 0.5 mm or less.

As the beam intensity increases for higher power operation, the beam emittance from the ECR ion source is possibly larger. In preparation for the larger emittance, we are planning to replace the 9 quadrupoles around the stripper (section "A" in Fig. 1) to allow the beam size to be maintained to a similar level or to enable further focusing of the beam with smaller emittances. The beam dynamics simulation shows that a larger aperture and stronger focusing quadrupoles are necessary to keep the beam size small at the stripper without beam loss on the quadruples. The currently installed 50-mm-bore quadrupoles (Q1-type) will be replaced with 75-mm-bore quadrupoles (Q2-type). The beam size was calculated by FLAME with various normalized emittance from 0.1 to 0.3 π-mm-mrad and turned out that we can keep same beam size even if the emittance increases by 50% or reduce beam size by 30% at same emittance as shown in Fig. 8. At the same time, we will also install a 15-mm-radius collimator just after the stripper module to eliminate large-scattered particles produced by the stripper.

Content from this work may be used under the terms of the CC BY 4.0 licence (© 2025). Any distribution of this work must maintain attribution to the author(s), title of the work, publisher, and DOI.

ISBN: 978-3-95450-260-8 ISSN: 2673-5547 doi: 10.18429/JACoW-HIAT2025-TUZ02

Content from this work may be used under the terms of the CC BY 4.0 licence (© 2025). Any distribution of this work must maintain attribution to the author(s), title of the work, publisher, and DOI.

After the replacement is completed, two replaced Q1-type quadrupoles will be installed upstream of the LS2 (section "B" in Fig. 1) and four will be upstream of the LS3 (section "C" in Fig. 1) to obtain additional knobs for transverse matching of multi-q beams. The placement of new quadrupoles has already been optimized by FLAME simulations for measured $^{238}U^{5q}$ CS parameters.

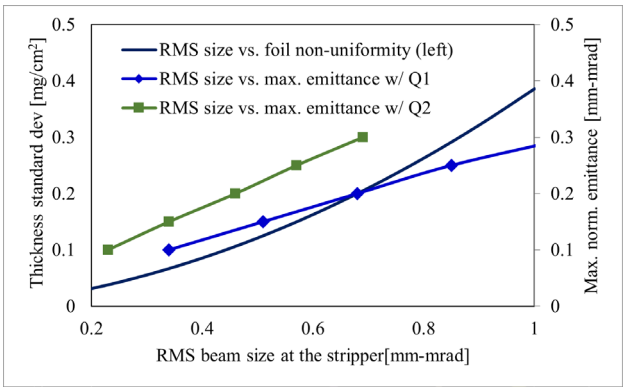


Figure 8: Li film thickness nonuniformity as a function of RMS beam size (black). Maximum normalized emittance allowing to reach the beam size on the stripper with current quadrupoles (blue) and larger aperture quadrupoles (green).

Installation of Second Harmonic Cavities

The feedback systems to compensate for post-stripper energy and energy loss at LLCS are beneficial in reducing the beam losses in LS2 cryomodules, but further mitigation is required to deliver 100 kW-level beams to the target.

After the beam passes through the LLCS, the so-called Landau tail describes its low energy distribution due to significant energy transfer by a single collision. The left side plot of Fig. 9 is the longitudinal acceptance for the $^{124}Xe^{3q}$ beam at the LLCS. The ions are lost in the LS2 if not in the white area after the stripper. The black points are simulated ^{124}Xe beam particles. These particles are simulated from the LEBT through the stripper. Then the energy loss of each particle is calculated by SRIM [9] using a measured lithium film thickness distribution. The low energy side of the acceptance is close to the beam, and possibly the Landau tail is out of the acceptance. The right plot in Fig. 9 is the acceptance with 2nd harmonics bunchers installed behind each of the current 161 MHz bunchers. The energy acceptance is significantly expanded.

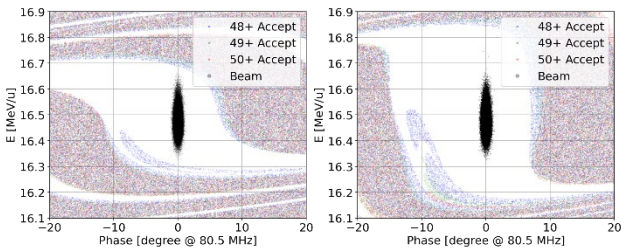


Figure 9: Simulated longitudinal phase-space acceptance at the stripper for $^{124}Xe^{3q}$ without (left) and with (right) second-harmonic cavities and beam (black).

Installation of New Wire Profile Monitors

Profile monitor scans for CS parameters calculation are one of the most time-consuming procedures during a PDT. The profile monitor at the matching sections is scanned with at least six different quadrupole settings for each charge state to calculate the CS parameters on x-x' and y-y' phase spaces. The measurement time is linearly proportional to the number of charge states. To make this procedure faster, we plan to install three profile monitors in the LS3 BTS (section "D" in Fig. 1). This section is a periodic FODO lattice with a 60° transverse phase advance per period. These profile monitors will be installed in the middle between the quadrupole doublets. Figure 10 shows the simulated rms beam ellipses on x-x' (top) and y-y' (bottom) with constraints imposed by the profile monitor measurements for $^{238}U^{5q}$.

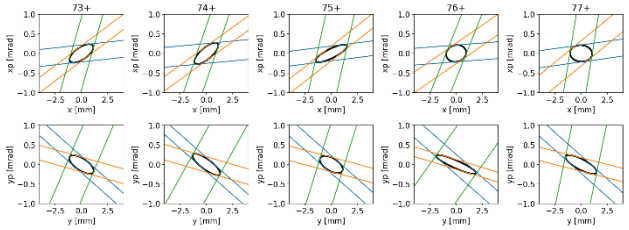


Figure 10: RMS beam ellipse on x-x' (top) and y-y' (bottom) for each of $^{238}U^{5q}$ beam and constraints imposed by three profile monitor measurements in LS3 BTS.

SUMMARY

FRIB linac routinely delivers 20 kW ion beams to the target from oxygen to uranium. We maintain uncontrolled beam losses at the level of 10^{-4}. At the current beam power level, these losses are well below 1 W/m which is an acceptable value for high power proton linacs. There is a hypothesis that the beam losses in the superconducting cavities can cause field emissions. Therefore, we keep the beam losses in the post-stripper linac about two orders of magnitude lower than 1 W/m. Recently, accelerator tunes have been developed for $^{238}U^{5q}$ and $^{48}Ca^{2q}$ beams characterized by low beam losses and suitable for higher beam power. The recent implementation of fast energy feedback and slow LLCS stage feedback reduced the beam losses in the LS2 cryomodules, which is good progress toward the next beam power level of 50 kW. Accelerator improvement projects are ongoing to mitigate further beam losses related to the LLCS, shorten the PDT, and increase science time.

REFERENCES

[1] J. Wei *et al.*, "Accelerator commissioning and rare isotope identification at the Facility for Rare Isotope Beams," *Mod. Phys. Lett. A*, vol. 37, no. 09, p. 2230006, Mar. 2022. doi:10.1142/s0217732322300063

[2] P. N. Ostroumov *et al.*, "Heavy ion beam physics at Facility for Rare Isotope Beams," *IEEE Open J. Instrum. Meas.*, vol. 15, no. 12, pp. P12034, Dec. 2020. doi:10.1088/1748-0221/15/12/p12034

[3] T. Kanemura *et al.*, "Experimental demonstration of the thin-film liquid-metal jet as a charge stripper," *Phys. Rev. Lett.*,

ISBN: 978-3-95450-260-8 ISSN: 2673-5547 doi: 10.18429/JACoW-HIAT2025-TUZ02

vol. 128, no. 21, p. 212301, May 2022. doi:10.1103/physrevlett.128.212301

[4] P. N. Ostroumov *et al.*, "First simultaneous acceleration of multiple charge states of heavy ion beams in a large-scale superconducting linear accelerator," *Phys. Rev. Lett.*, vol. 126, no. 11, p. 114801, Mar. 2021. doi:10.1103/physrevlett.126.114801

[5] A. S. Plastun and P. N. Ostroumov, "Instant phase setting in a large superconducting linac", in *Proc. NAPAC'22*, Albuquerque, NM, USA, Aug. 2022, pp. 885-890. doi:10.18429/JACoW-NAPAC2022-THZD1

[6] T. Zhang *et al.*, "Physics Applications in Support of FRIB Beam Tuning and Operations", presented at HIAT'25, East Lansing, MI, USA, Jun. 2025, paper MOP21, this conference.

[7] Zhao *et al.*, "BPM feedback for LLRF energy and phase regulation in charge stripping beamlines", in *Proc. IPAC'24*, Nashville, TN, USA, May 2024, pp. 3326-3328. doi:10.18429/JACoW-IPAC2024-THPG32

[8] P. N. Ostroumov *et al.*, "Acceleration of uranium beam to record power of 10.4 kW and observation of new isotopes at Facility for Rare Isotope Beams," *Phys. Rev. Accel. Beams*, vol. 27, no. 6, p. 060101, Jun. 2024. doi:10.1103/physrevaccelbeams.27.060101

[9] J. F. Ziegler, M. D. Ziegler, and J. P. Biersack, "SRIM – The stopping and range of ions in matter (2010)," *Nucl. Instrum. Methods Phys. Res., Sect. B*, vol. 268, no. 11–12, pp. 1818–1823, Jun. 2010. doi:10.1016/j.nimb.2010.02.091

Content from this work may be used under the terms of the CC BY 4.0 licence (© 2025). Any distribution of this work must maintain attribution to the author(s), title of the work, publisher, and DOI.